Interface-driven conductance transition in nanostructured polymer networks

O. O. Adetunji,[1] N.-R. Chiou,[2] and A. J. Epstein[1,2,*]
[1]*Department of Physics, The Ohio State University, Columbus, Ohio 43210-1117, USA*
[2]*Department of Chemistry, The Ohio State University, Columbus, Ohio 43210-1180, USA*
(Received 19 June 2009; published 13 July 2009)

We report an anomalous electronic transport signature in polyaniline nanofiber networks probed via the temperature-dependent dc conductivity $[\sigma_{dc}(T)]$, reflectance $[R(\omega,T)]$ over a broad frequency range (300–50 000 cm^{-1}), and x-ray diffraction. We determined that disorder and localization dominate the bulk charge dynamics and propose that the origin of the atypical electronic transport signature in the nanofibers networks is the "fragile" nature of the conductance at the nanofiber interfaces resulting from the strong T-dependent localization of electronic states in the nanostructure interface regions.

DOI: 10.1103/PhysRevB.80.012201 PACS number(s): 72.80.Le, 61.05.cp, 72.20.Ee, 78.30.Jw

The electronic properties of nonporous polyaniline films prepared by conventional polymerization[1] have been extensively studied[2] through optical,[2–6] charge transport,[2,5,7–9] structural,[10–12] and magnetic probes.[12,13] Though these films are typically between 10% and 50% crystalline with coherence lengths of several nm, electron micrographs reveal these films as smooth and featureless due to the presence of the amorphous polyaniline essentially coating the surface and extending into the bulk of the film. The σ_{dc} of dense film samples that contain extensively disordered regions is dominated by hopping at all temperatures. Samples with less disorder have metal-like signatures at high temperature (typically $T>200$ K), with a broad maximum in $[\sigma_{dc}(T)]$ and with a change in conductivity from room temperature (RT) to the broad conductivity maximum of $\sim 15\%$, and a clear localized transport at low temperatures.[5,12]

In recent years, the progress in controlled synthesis has led to the fabrication of networks of polyaniline nanofibers and nanotubes,[14–21] with tunable nanofiber and nanotube diameters. The films of polyaniline nanofibers networks (PAN-nfNs) charge transport being reported here behave differently than metallic or dielectric conventional polyaniline and different from metallic or dielectric single nanotubes of polyaniline.[5,8,14] The films of PAN-nfN have anomalous transport properties requiring a new approach to understanding their transport behavior. The PAN-nfN conductivity increases by >200% as the PAN-nfN is cooled from room temperature to 235 K—very different than the behavior earlier reported for any metallic polyaniline. These differences are summarized in Table I. A recent charge transport study of a polyaniline nanofiber network also showed a similar sharp maximum around 230 K and a large conductivity increase from RT to the maximum conductivity. The $[\sigma_{dc}(T)]$ behavior was assigned[18] to that of a metallic transport similar to that of conventional metallic polyaniline. However, the study did not provide results of related experiments to determine the mechanisms governing charge-carrier motion in the interconnected network. Doped polyaniline nanofiber networks are model systems to study the nature of charge carriers within this nanostructure polymer network topology. In order to understand the origin of the anomalous transport characteristics in PAN-nfN including the sharp maximum at 235 K, we probed the PAN-nfN using a wide variety of experiments to determine the mechanisms governing this unusual phenomenon.

In this Brief Report, we report the conductivity at dc (30–300 K), the frequency and temperature dependence of the dielectric constant $[\varepsilon(\omega,T)]$ of the nanofibers network over very broad frequency (300–50 000 cm^{-1}) and temperature ranges (20–300 K) derived from the Kramers-Kronig analysis of the reflectance combined with the x-ray diffraction (XRD) of the PAN-nfN and pressured PAN-nfN films. Application of modest pressure (4000 psi) is shown to irreversibly change the fiber morphology and the electronic response while leaving the x-ray structures the same. The results of these experiments led us to conclude that the PAN-nfN is not metallic and to propose that the behavior of PAN-nfN is the first proposed example of an "interface-driven conductance transition" in a nanostructured conducting polymer network.

The PAN-nfN samples studied here were prepared via dilute polymerization with ClO_4^- as the dopant following our earlier published procedure.[16] The doping level of the resulting polyaniline nanostructure measured by the perchlorate to nitrogen ratio from the elemental analysis was 28%. The $\sigma_{dc}(T)$ measurement were performed on PAN-nfN and pellet PAN-nfN films using a standard four-probe technique. The dc conductivity was measured in a Quantum Design physical property measurement system (PPMS)-9 platform with an addition sample probe Keithley 2400 Sourcemeter. PAN-nfN was drop cast onto a glass substrate containing four gold patterned electrodes; the separation between the gold electrodes was 2 mm and the width of each electrode was 0.5 mm. The PAN-nfN pellet sample prepared at a pressure of 4000 psi was mounted on a glass substrate using Kapton tape (3M™ Polyimide 1205). Four copper wires (0.05 mm in diameter) were connected parallel to the pellet PAN-nfN sample surface with graphite paint (Acheson Electrodag 502) to ensure good electrical contact. For both PAN-nfN and pellet PAN-nfN films, the current was applied through the outer electrodes/wires, while the voltage drop was measured across the inner two electrodes/wires. The dissipative power was kept under 10^{-7} W to eliminate self-heating effects. The T and ω dependences of reflectance was measured using a Bruker IFS 66v/S Fourier transform infrared spectrometer equipped with a continuous flow He cryostat over the range 300–50 000 cm^{-1}. The high-energy (5000–50 000 cm^{-1})

TABLE I. Summary of reported differences in the electronic transport of conventional polyaniline films(PAN), single polyaniline nanofiber(PAN-nf), polyaniline nanofiber network films(PAN-nfN) and single polyaniline nanotube(PAN-nt).

	Conventional polyaniline		Nanostructured polyaniline		
Polyaniline (PAN)	Metallic PAN[a–c]	Disordered PAN[d]	PAN-nf	PAN-nfN (This work)	PAN-nt[e]
σ_{dc}(RT)	$\sigma_{dc}(\mathrm{RT}) > \sim 80$ S/cm	$\sigma_{dc}(\mathrm{RT}) < \sim 80$ S/cm	There is no report	$\sigma_{dc}(\mathrm{RT}) < \sim 1$ S/cm	$\sigma_{dc}(\mathrm{RT}) \sim 32$ S/cm
Behavior of $[\sigma_{dc}(T)]$	$[\sigma_{dc}(T)]$ increases as T is decreased from RT to a broad maximum ~ 210 K	$[\sigma_{dc}(T)]$ decreases as T is decreased from RT with no maximum	There is no report	$[\sigma_{dc}(T)]$ increases as T is decreased from RT to a sharp maximum ~ 235 K	$[\sigma_{dc}(T)]$ decreases as T is decreased from RT with no maximum
The change in σ_{dc} from RT to maximum	σ_{dc} change from RT to the broad $[\sigma_{dc}(T)]$ maximum is $\sim 15\%$	No maximum for $[\sigma_{dc}(T)]$	There is no report	σ_{dc} change from RT to the sharp conductivity maximum is $\sim 200\%$	No maximum for $[\sigma_{dc}(T)]$
$\varepsilon(\omega, T)$ Signature at the plasma frequency	The $\varepsilon(\omega, T)$ crosses zero signifying that the charge carriers are delocalized	The $\varepsilon(\omega, T)$ does not cross zero signifying that the charge carries are localized	There is no report	The $\varepsilon(\omega, T)$ does not cross zero signifying that the charge carries are localized	There is no report on PAN-nt $\varepsilon(\omega, T)$

[a]Reference 5.
[b]Reference 25.
[c]Reference 26.
[d]Reference 4.
[e]Reference 14.

FIG. 1. (a) The scanning electron micrograph (SEM) of polyaniline nanostructures obtained by 1M $HClO_{4(aq)}$ dilute polymerization. (b) The corresponding SEM image after the application of 4000 psi pressure to the nanostructure.

reflectance was measured at RT using a Varian Cary 5000 spectrometer equipped with an integrating sphere. The RT reflectance at low energy (300 cm^{-1}) was $\sim 50\%$ and the reflectance at low energies decreased with decreasing temperature. For energies below 300 cm^{-1}, the reflectance was assumed to be constant, between 50 000–100 000 cm^{-1} the reflectance was assumed to fall off as $\frac{1}{\omega^2}$, and above 100 000 cm^{-1}, the extrapolation was taken as $\frac{1}{\omega^4}$.[22] To correct for diffuse scattering due to the roughness of the film, the gold overcoating method[23] was used for scaling the low-energy measurement. Structural XRD experiments were performed using an x-ray scanning diffractometer [Rigaku Ultima-III, with a Cu $K\alpha$ radiation source ($\lambda = 1.542$ Å)]. Pressure of 4000 psi was applied to the PAN-nfN using a K Br pellet press (Carver Laboratory Equipment, Hydraulic Unit model 3912).

Table I shows the reported differences between the electronic transport of conventional polyaniline, single polyaniline nanotube, and polyaniline nanofiber network films. Figure 1 shows the scanning electron microscope images of the nanostructure sample before and after the application of pressure. The application of 4000 psi of pressure to PAN-nfN changes the morphology to that of a continuous film. The σ_{dc}(RT) of the PAN-nfN film is ~ 0.7 S/cm, ~ 100-fold smaller than the Mott minimum metallic conductivity (MMMC). The σ_{dc}(RT) for the pressed PAN-nfN is ~ 3-fold larger than that of the PAN-nfN similar to the 0.7 S/cm for the PAN-nfN when corrected for the presence of $\sim 2/3$ voids, but still well below the MMMC (Refs. 4, 8, and 24) [Fig. 2(a)]. For the PAN-nfN film, σ increased rapidly as the temperature decreased from RT until ~ 235 K. Below that, a gradual decrease in σ was noted as the temperature was reduced to ~ 30 K. The reduced activation energy W

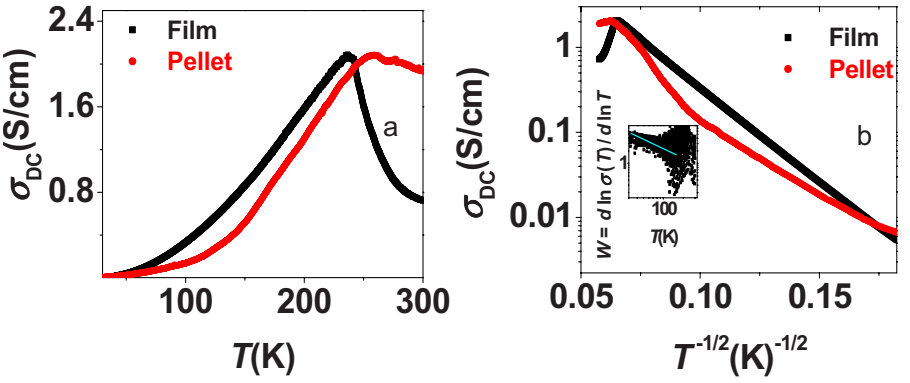

FIG. 2. (Color online) (a) $\sigma_{dc}(T)$ for polyaniline nanostructure and pressed polyaniline nanostructure as a function of temperature. (b) ln σ_{dc} vs $T^{-1/2}$ of dc conductivity of $HClO_4$ doped nanostructure polyaniline; the filled bold black square is for the nanostructure film while the filled red circle is for the nanostructure pressed film(pellet). The inset is the reduced activation energy (W) vs T for the nanostructure film (cyan line is just a straight-line guide).

$\equiv d \ln \sigma_{dc}(T)/d \ln T$ vs T (Refs. 2, 5, 7, and 8) is presented in the inset of Fig. 2(b). The charge transport dynamics for the PAN-nfN film and pellet both follow a quasi-one-dimensional (quasi-1D) variable range-hopping (VRH) model,[9,12] where $\sigma_{dc} \propto \exp[(-\frac{T_0}{T})^{1/2}]$, and T_0 can be interpreted as an effective energy barrier between localized states determined by the degree of disorder. The onset of the quasi-1D VRH for the nanostructured film is just below $T_{\max} \sim 235$ K (we have seen similar quasi-1D VRH behavior in other PAN-nfN doped with hydrochloric acid and with camphorsulfonic acid); while for the pressed nanostructured pellet, the model holds for $T < 100$ K.

Optical studies [Fig. 3(a)] showed reflectance approaching 50% at 300 cm^{-1}. The oscillations in the mid-IR (500–2500 cm^{-1}) are assigned to phonons and there was no significant change in the mid-IR signature over T-range studied. For all measured temperature ranges, the optical dielectric constants [Fig. 3(b)] were calculated from the Kramers-Kronig analysis.[22] The optical dielectric constants did not cross zero, suggesting that the plasma response was overdamped ($\Omega_P \tau \sim 1$). To calculate the T-dependent dielectric constants, the low-T reflectance data were extrapolated to higher energy using the RT reflectance.

X-ray diffraction studies [inset of Fig. 3(b)] indicated that the PAN-nfN and pellet PAN-nfN films were ~50% crystalline, with a coherence length of ~2 nm. This coherence length is similar to the values reported earlier for conventional polyaniline with less disorder and higher conductivity.[10] We suggest that due to the average diameter size of the nanostructure fiber (~40 nm), which is a factor of 20 more than the coherence length, the XRD probes partially crystalline regions similar to bulk conventional polyaniline.

The signature of $[\sigma_{dc}(T)]$ features an anomalous electronic transport signature characterized by conductivity increasing by a factor of 3 as the PAN-nfN is cooled from RT to 235 K. The σ_{dc}(RT) of the PAN-nfN (~0.7 S/cm) is very small compared to the MMMC. Therefore, we expect the charge transport of the PAN-nfN to be dominated by phonon activation with very little or no metallic contribution. On the contrary, the charge transport of PAN-nfN films increases as the temperature is lowered from RT to ~235 K. However, for the pressed PAN-nfN films, the polymer nanofibers merge as 4000 psi pressure is applied leading to continuous film morphology. The signature of the charge transport for the pressed PAN-nfN films resembled that of conventional disordered polyaniline,[4] having a broad peak and a moderate change in conductivity from σ_{dc}(RT) to the peak conductivity.

Based on the wide range of experimental results presented here, we propose that the charge transport of the PAN-nfN films is affected by two competing mechanisms: the interactions with phonons in the bulk of each nanofiber and the nature of the conductance at the nanofiber-nanofiber interfaces. We propose at low temperatures, below <235 K the effect of "fragile" (consisting mainly of weakly intertwined nanofibers interface susceptible to becoming broken, loose, and disconnected from each other) interfiber contacts is small, while the effect of phonon activation dominates the charge transport dynamics, so electrons can hop from one localized state to another. As higher temperatures are approached, the effect of phonon assistance is reduced, and the fragile nature of the interfiber contact dominates, leading to a longer charge transport path length and a more resistive nanostructure network as the temperature is increased above 235 K. In contrast, with the pressed PAN-nfN, the applied pressure significantly reduced the effect of interfiber contacts

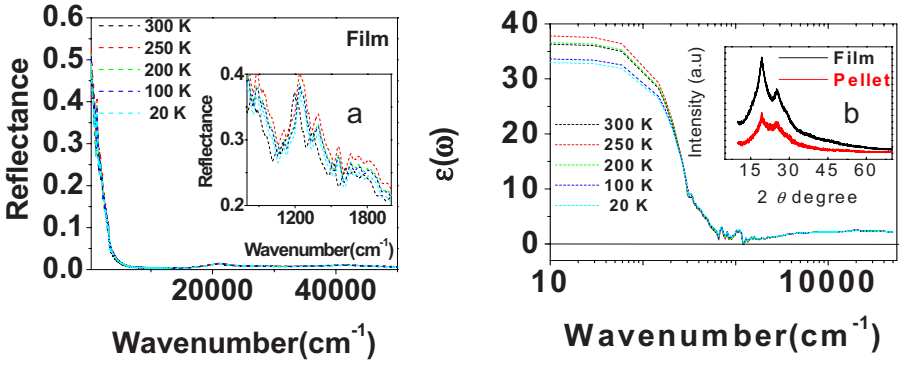

FIG. 3. (Color online) (a) The temperature-dependent reflectance of polyaniline nanostructure film. Inset is the optical reflectance in the mid-IR frequencies of the nanostructure film. (b) The dielectric function of the nanostructure film. Inset shows the RT XRD measurements of the nanostructure film and pressured nanostructure.

leading to a shorter charge transport path length as the morphology was transformed from one consisting of nanofibers to that of a continuous film. Therefore, the signature of charge transport resembled that of a conventional polyaniline pellet with disorder. From the fit of $\ln \sigma_{dc}$ vs $T^{-1/2}$ to a 1D VRH model, we estimate T_0 as $\sim 2.5 \times 10^3$ K for the film and $\sim 1.39 \times 10^3$ K for the pellet, similar to reported values for disordered polyaniline films.[12] These values suggest that the PAN-nfN film had a greater degree of disorder in the disordered regions compared to the pellet (pressed) PAN-nfN film. The increase in W with decreasing T implies that the system is in the insulating regime throughout the temperature range studied. The dielectric functions $\varepsilon(\omega, T)$ also revealed that the charge carriers were localized, similar to the result of the reduced activation energy plot W. The RT XRD measurement indicated a $\sim 50\%$ crystalline sample. However, due to the fragile nature of the nanofiber interface contacts, the effective conductivity of the network was significantly reduced.

In summary, the $[\sigma_{dc}(T)]$ transport data of PAN-nfN exhibit an anomalous electronic transport signature behaving differently from conventional polyaniline and polyaniline nanotube, while pressed PAN-nfN exhibits charge transport signature typical of conventional polyaniline. The dielectric constant revealed that the charge carriers within the nanofiber network are localized. RT XRD data showed a partially crystalline PAN-nfN; however, the effective conductivity of the network is less than the MMMC. Therefore, our experimental results suggest that the anomalous electronic behavior seen in the signature of the temperature-dependent dc conductivity of the PAN-nfN is driven by the fragile nature of conductance at the nanostructured interface, while disorder and localization dominate the bulk charge dynamics.

We thank V. N. Prigodin for useful discussions. This work was supported in part by the NSF-IGERT under Grant No. DGE- 0221678 and the NSF-NSEC under Grant No. EEC-0425626. This work was also supported in part by The Ohio State University Institute for Materials Research.

*epstein@mps.ohio-state.edu

[1] A. G. MacDiarmid, J.-C. Chiang, A. F. Richter, N. L. D. Somasiri, and A. J. Epstein, in *Conducting Polymers*, edited by L. Alcacer (Reidel, Dordrecht, 1987), Vol. 105; A. G. MacDiarmid, J.-C. Chiang, A. F. Richter, and A. J. Epstein, Synth. Met. **18**, 285 (1987).

[2] A. J. Epstein, in *Handbook of Conducting Polymers*, edited by T. A. Skotheim and J. R. Reynolds, 3rd ed. (CRC Press/Taylor & Francis Group, Boca Raton, FL, 2007).

[3] S. Stafström, J. L. Brédas, A. J. Epstein, H. S. Woo, D. B. Tanner, W. S. Huang, and A. G. MacDiarmid, Phys. Rev. Lett. **59**, 1464 (1987).

[4] R. S. Kohlman, J. Joo, Y. G. Min, A. G. MacDiarmid, and A. J. Epstein, Phys. Rev. Lett. **77**, 2766 (1996).

[5] R. S. Kohlman, A. Zibold, D. B. Tanner, G. G. Ihas, T. Ishiguro, Y. G. Min, A. G. MacDiarmid, and A. J. Epstein, Phys. Rev. Lett. **78**, 3915 (1997).

[6] K. Lee, A. J. Heeger, and Y. Cao, Phys. Rev. B **48**, 14884 (1993).

[7] J. Joo, V. N. Prigodin, Y. G. Min, A. G. MacDiarmid, and A. J. Epstein, Phys. Rev. B **50**, 12226 (1994).

[8] Reghu Menon, C. O. Yoon, D. Moses, A. J. Heeger, and Y. Cao, Phys. Rev. B **48**, 17685 (1993).

[9] J. Joo, Z. Oblakowski, G. Du, J. P. Pouget, E. J. Oh, J. M. Wiesinger, Y. G. Min, A. G. MacDiarmid, and A. J. Epstein, Phys. Rev. B **49**, 2977 (1994).

[10] J. P. Pouget, M. E. Jozefowicz, A. J. Epstein, X. Tang, and A. G. MacDiarmid, Macromolecules **24**, 779 (1991).

[11] M. Laridjani, J. P. Pouget, E. M. Scherr, A. G. MacDiarmid, M. E. Jozefowicz, and A. J. Epstein, Macromolecules **25**, 4106 (1992).

[12] J. Joo, S. M. Long, J. P. Pouget, E. J. Oh, A. G. MacDiarmid, and A. J. Epstein, Phys. Rev. B **57**, 9567 (1998).

[13] J. M. Ginder, A. F. Richter, A. G. MacDiarmid, and A. J. Epstein, Solid State Commun. **63**, 97 (1987).

[14] Y. Long, Z. J. Chen, N. L. Wang, Y. J. Ma, Z. Zhang, L. J. Zhang, and M. X. Wan, Appl. Phys. Lett. **83**, 1863 (2003).

[15] N.-R. Chiou and A. J. Epstein, Synth. Met. **153**, 69 (2005).

[16] N.-R. Chiou and A. J. Epstein, Adv. Mater. **17**, 1679 (2005).

[17] N. R. Chiou, L. J. Lee, and A. J. Epstein, J. Mater. Chem. **18**, 2085 (2008).

[18] P. Dallas, D. Stamopoulos, N. Boukos, V. Tzitzios, D. Niarchos, and D. Petridis, Polymer **48**, 3162 (2007).

[19] J. Huang, S. Virji, B. H. Weiller, and R. B. Kaner, J. Am. Chem. Soc. **125**, 314 (2003).

[20] X. Zhang, W. J. Goux, and S. K. Manohar, J. Am. Chem. Soc. **126**, 4502 (2004).

[21] N.-R. Chiou, L. Cui, J. J. Guan, L. J. Lee, and A. J. Epstein, Nat. Nanotechnol. **2**, 354 (2007).

[22] F. Wooten, *Optical Properties of Solids* (Academic, New York, 1972).

[23] A. Ugawa, A. G. Rinzler, and D. B. Tanner, Phys. Rev. B **60**, R11305 (1999); C. C. Homes, M. Reedyk, D. A. Crandles, and T. Timusk, Appl. Opt. **32**, 2976 (1993).

[24] N. F. Mott and E. Davis, *Electronic Processes in Non-Crystalline Materials* (Clarendon Press, Oxford, 1979).

[25] A. N. Aleshin, K. Lee, J. Y. Lee, D. Y. Kim, and C. Y. Kim, Synth. Met. **99**, 27 (1999).

[26] M. Reghu, Y. Cao, D. Moses, and A. J. Heeger, Phys. Rev. B **47**, 1758 (1993).